Biomedical Microdevices (2021) 23: 9
https://doi.org/10.1007/s10544-021-00545-4

Optimization, fabrication, and characterization of four electrode-based sensors for blood impedance measurement

Rangadhar Pradhan[1] · Sanjana Afrin Raisa[2] · Pramod Kumar[2] · Ashish Kalkal[3] · Narendra Kumar[2] · Gopinath Packirisamy[1,3] · Sanjeev Manhas[2]

Accepted: 5 January 2021 / Published online: 15 January 2021

Abstract

In this work, an optimized, non-invasive four electrode-based impedimetric sensors have been designed, fabricated, and characterized for measuring the impedance of a biological cell. The impedimetric sensors having four mono-polar electrodes were fabricated utilizing the photolithography technique with gold as the electrode material. Furthermore, the impedance of the electrolyte/electrode interface was simulated by optimizing different parameters, including applied voltage, PBS thickness, and diameter, using COMSOL Multiphysics software for a frequency range of 100 Hz to 1 MHz. Next, the impedance of the fabricated device was measured experimentally using the electrochemical impedance spectroscopy (EIS) technique. Then, the COMSOL data was equated with the impedance obtained from the fabricated devices to realize the feasibility and error percentage (RSE < 5%) of the sensor. The equivalent circuit model for the measured impedance data of PBS was obtained utilizing the ZsimpWin software. Besides, the mathematical relations between the impedance, phase angle and the area of the electrode were interpreted for the fabricated impedimetric sensors. Later on, a real blood sample was also characterized to demonstrate the feasibility and the validity of the proposed technique and the fabricated devices in cell diagnosis.

Keywords EIS · COMSOL multiphysics · ZsimpWin · Sensor · Blood impedance

1 Introduction

The invention of the electrode-based impedimetric sensor is indeed a significant breakthrough in the research arena of microelectronics, nanotechnology, and bio-electronic devices (Franks et al. 2005; Curtis et al. 2009; Kumar et al. 2018a). It opened the pathway to in-depth studies on the functionality of living cells, both qualitatively and quantitatively. Hence, it promises a reliable technique in the field of cancer research (Hong et al. 2011; Láng et al. 2017; Pradhan et al. 2014a; Kalkal et al. 2020), cell behavior measurement (Xiao et al. 2002; Wang et al. 2010; Pradhan et al. 2014b), and drug discoveries (Huang et al. 2003; Giaever and Keese 1993; Pradhan et al. 2014c) as well as cytotoxity (An et al. 2019; Pradhan et al. 2014d), quantification of barrier formation (Szulcek et al. 2014; Benson et al. 2013; Schmiedinger et al. 2020), and wound healing (Cavallini and Tarantola 2019). Dr. Ivar Giaever and Dr. Charles R. Keese invented this impedance-based cell monitoring technology in the early 1980s. They used fabricated gold electrodes for monitoring cell movement and to monitor the barrier formation of a cell (Giaever and Keese 1993; Giaever and Keese 1984; Giaever and Keese 1991; Giaever and Keese 2000). The particular device acts as a transducer that changes the biological/chemical signal into an electrical signal. In this technique, living cells are grown on the top of the conductive metal electrodes, preferably of gold, silver, or platinum. The living cell acts as an insulator due to the inherent insulating properties of its cell membrane and cytoplasm (Raicu et al. 2008). A biological cell contains intracellular fluids (ICF), cell membranes with or without a cell wall, and suspended extracellular

Rangadhar Pradhan, Sanjana Afrin Raisa and Pramod Kumar contributed equally to this work.

✉ Rangadhar Pradhan
rangadhar@gmail.com

✉ Sanjeev Manhas
sanjeev.manhas@ece.iitr.ac.in

[1] Center for Nanotechnology, Indian Institute of Technology Roorkee, Roorkee 247667, India

[2] Department of Electronics & Communication Engineering, Indian Institute of Technology Roorkee, Roorkee 247667, India

[3] Department of Biotechnology, Indian Institute of Technology Roorkee, Roorkee 247667, India

fluids (ECF). When a small alternative current (AC) (10^2–10^6 Hz) passes through the cell, the cell membrane and cytoplasm of the cell creates hindrance in the transmission of the current that is recorded in a phase-sensitive impedance measurement instrument. From the variation in the measured impedance of the cell, the shape, characteristics, and behavior of the living cell can be known (Chang and Park 2010; Hu et al. 2013). This is because the cell produced a complex bioelectrical impedance under AC excitation, which further depends on the cell compositions and the frequency (Ackmann 1993). A minimal change in the cell composition will be reflected in the bio-impedance; therefore, the biological cell impedance is an effective way of cell diagnosis.

The electrochemical impedance spectroscopy (EIS) technique consists of 2, 3 & 4 electrodes configurations. Out of them, a 3-electrodes system is the most common configuration. It mainly comprises of Working Electrode (the sensing electrode embedded in working electrode) (WE), Reference Electrode (RE), and Counter Electrode (CE) (Kumar et al. 2018b; Pradhan et al. 2019; Orazem and Tribollet 2017). The WE passes the AC to the sample under test; that current is collected by CE (sink), thereby completing the whole circuit, whereas the RE provides a constant voltage as a reference. For the present study, the sensing electrode has been separated from the working electrode, providing an extra electrode for improving the sensing capability of the whole impedimetric device. The present sensor in this research has four electrodes - Working Electrode (WE), Reference Electrode (RE), Counter Electrode (CE), and a Sensing Electrode (SE). Here, the impedance was obtained by applying a small AC through the WE and CE electrodes, and the output impedance is measured from the SE (Brom-Verheijden et al. 2018). In a 3-electrode setup, the same electrode is used as the working and sensing electrode which is prone to noises in the output signal. Whereas, it is separated in the case of 4-electrode setup. Therefore, the noise level reduces in the output signal (Xia et al. 2020). Moreover, this kind of setup is the perfect choice for measuring impedance across solution-phase interface, such as a membrane or liquid-liquid junction, which is the case in bioimpedance.

The microelectronic device has several advantages of being label-free, non-invasive, portable, cost-effective, reduced sample volume, higher current density. These devices ensure higher accuracy and real-time monitoring, which are significant for biomedical researches (Park and Shuler 2003; Pradhan et al. 2012; Srinivasaraghavan et al. 2014). However, the noise due to interfacial capacitance is deemed as a critical drawback of the microelectrode devices (Franks et al. 2005; Pradhan et al. 2014b; Pradhan et al. 2012). Meanwhile, the complete removal of this interfacial noise is highly unlikely; the reduction in the parasitic capacitance is necessary to minimize the noises in the measured data. Considering this fact, the optimization for its parameters of the impedimetric device, such as electrode area, thickness, and diameter of electrolyte, and the applied voltage is essential to get the exact impedance of the whole system (Lai et al. 2019). The EIS (electrical impedance spectroscopy) has already been established as non-invasive sensing techniques, and researchers all over the world have used this technique for glucose monitoring (Huang et al. 2020), cell diagnosis (Filho et al. 2018; Bera 2014). The present work has also demonstrated a 4-electrode prototype of the device used in non-invasive cell diagnosis purposes. The AC used in the experiment does not harm or destroy the cell; therefore, the technique can be termed as non-invasive.

For the first time, this article reports the optimization studies of the 4-electrode-based devices for impedance measurement. The optimization of the interfacial layer was done by simulating diverse design parameters to employ the final device better. All the proposed sensors were simulated by using COMSOL Multiphysics, and later the simulated data were matched with the investigational data of the fabricated device for phosphate-buffered saline (PBS). The impedimetric devices were fabricated by e-beam deposition and standard photolithography techniques. Subsequently, the electrical parameters are obtained from the experimental data by using a suitable equivalent circuit. A mathematical relationship was developed between the impedance, phase angle, and the area of the working electrode for PBS. Also, these devices were used to measure blood impedance successively.

2 Optimization of Impedimetric device

2.1 Design of electrode

This study shows the effects of the sensor geometry on the output impedance signal of the sample. The aim is to minimize the parasitic double-layer capacitance generated by the polarization effect at the electrode/electrolyte interface (Padmaraj et al. 2011). This capacitance becomes significant for the biological samples, as the conductivity of the buffer solution is very high. As stated in their work (Franks et al. 2005; Pradhan et al. 2012), the double-layer capacitance formation can be prevented by keeping the inactive electrode area and the substrate separated from the electrolytic solution. Therefore, a coating of polymer or passivation layer (SU8) is applied to the connecting leads, and only the active electrode regions are exposed for sensing purposes (Pradhan et al. 2012; Price et al. 2009). The gold electrode used in the sensors is chosen for its chemically inert nature with the living cells; therefore, it does not affect the output impedance. In this work, the author used the 4- electrode technique with gold electrodes instead of the conventional 3-electrode technique to attain the maximum sensitivity of the device.

To avoid any cross-contamination between electrodes, all the electrodes are positioned at a distance of 100 μm from each other (Price et al. 2009). The geometrical dimensions of WE, SE, RE, CE for the four different designs are 50 × 50 μm, 100 × 100 μm, 150 × 150 μm; 200 × 200, as shown in Table 1. All the electrodes are connected to the contact pads (1000 μm × 1000 μm) via a 100-μm comprehensive interconnection line from which the external electrical input is supplied. For measuring the impedance of electrolyte, a cylinder-shaped well of 78.5 mm^2 area has been placed surrounding the active electrodes.

2.2 Procedure of optimization

Four design geometries (described above) for the impedimetric sensors were optimized by considering the different design parameters. For each design, simulations have been done varying the parameters like applied voltage (5 mV, 10 mV, 15 mV, 20 mV), the thickness of PBS solution (500 μm, 1000 μm, 1500 μm, 2000 μm), and the diameter of the circular PBS region (2000 μm, 4000 μm, 6000 μm and 8000 μm), as described in Table 2. For each simulation, only one parameter was varied, keeping the other two parameters constant in the COMSOL Multiphysics software. Finally, the simulation outputs were compared with the equivalent circuits in the ZsimpWin software, and the optimized design parameters were obtained.

2.3 Equations used in COMSOL multiphysics

The COMSOL Multiphysics software (version 5.2) has been used to simulate and optimize the design using the finite element method (FEM) and different numerical approaches. Here, the AC/DC module has been selected for conducting the simulations, and the electric current interface and a Frequency Domain study step are chosen for designing the electrodes. The simulation considered two assumptions, first was the linear and curl-free electric field, and the second one was the purely capacitive nature of the electrodes. The model uses the 2D time harmonics analysis of electric current for impedance analysis which operates on the assumption that the electric field is linear. Moreover, there is no magnetic field present at the electrodes; therefore, the inductive effect can be neglected. Thus the electric field can be expressed as the gradient of a scalar potential V, as discussed in (Pradhan et al. 2012). The continuity equation is described as follows:

$$-\nabla.(\sigma + j\omega\varepsilon_r\varepsilon_0)\nabla V = 0 \quad (1)$$

Where ε_r depicts relative permittivity, ε_0 denotes free space permittivity, V represents the voltage, $\boldsymbol{\omega}$ is the angular frequency, and $\boldsymbol{\sigma}$ is the conductivity of the system. The following equations represent the equations used for displacement D and electric field E:

$$E = -\nabla V \quad (2)$$

$$D = \varepsilon_0\varepsilon_r E \quad (3)$$

The module obtains the current density J using Ohm's law as below:

$$J = \sigma E + j\omega D + J_e \quad (4)$$

Where σ denotes the conductivity of the electrolyte PBS and Je is the external current density. Since in the system, no external current density was present, the equation could be reduced to:

$$J = \sigma E + j\omega D \quad (5)$$

2.4 Simulating parameters

The COMSOL Multiphysics software simulates four thin gold microelectrodes on a glass substrate, confined by a Pyrex cylinder containing 1 mL of PBS electrolytic solution. The PBS has a relative dielectric constant of 136 and a conductivity of 2×10^{-5} S/m (Wang and Jang 2009). The PBS layer, which has contact with the cylinder walls, has been considered as an insulator while all the four gold electrodes were modeled as the perfect electric conductors. The counter and reference electrodes have been set to ground potential, whereas the

Table 2 Parameters of optimization

Parameter	Step 1	Step 2	Step 3	Step 4
Voltage	5 mV	10 mV	15 mV	20 mV
PBS thickness	500 μm	1000 μm	1500 μm	2000 μm
PBS diameter	2000 μm	4000 μm	6000 μm	8000 μm

Table 1 Dimensions of the various designs

Designs	1	2	3	4
Dimension of the electrode	50×50 μm	100×100 μm	150×150 μm	200×200 μm
Connecting width	5 mm	5 mm	5 mm	5 mm
Bond pad	1×1 mm	1×1 mm	1×1 mm	1×1 mm

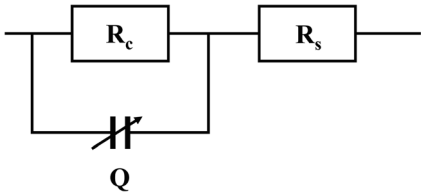

Fig. 1 Equivalent Circuit model used for the PBS experiment

working and sensing electrodes were provided with a terminal voltage of 5 mV, 10 mV, 15 mV, 20 mV, etc. for each set of simulations. Thus, an electric connection was built from the working electrode to the counter electrode, subsequently establishing an electric field.

2.4.1 Equivalent circuit simulation by using ZsimpWin

The simulated impedance values extracted from the COMSOL Multiphysics model were exported to ZsimpWin (Equivalent circuit simulator, Version 3.21) to validate the simulation (Pradhan et al. 2010; Pradhan et al. 2011). The equivalent circuit, as shown in Fig. 1 extracted from previous literature (Pradhan et al. 2012) was used to get the optimized parameters by fitting the COMSOL and ZsimpWin data, subsequently leading to the fabrication of a device to measure blood impedance. In the equivalent circuit, R_s represent solution resistance, R_c denotes charge transfer resistance, and Q represents double-layer capacitance for electrode/electrolyte interface.

Also, the values of different electrical parameters have been extracted from experimental data with the help of ZsimpWin software by several iterative processes in which the chi-square (χ^2) value plays a vital role in validating the equivalent circuit model (Boukamp 1989). The standard value of χ^2 has been found to be 1.5×10^{-3} or less well within the reported range (Pradhan et al. 2011).

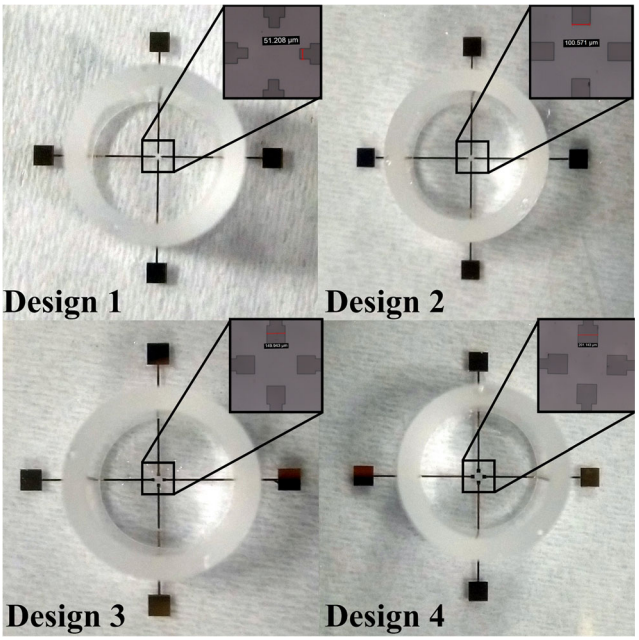

Fig. 3 Fabricated 4-electrodes based devices with cloning cylinder (inset: Microscopic view)

3 Device fabrication

The impedimetric devices have been fabricated on the glass substrate by using the photolithography technique (selective etching of the material deposited). Initially, thin layers of Titanium (100 Å) and gold (500 nm) were thermally deposited on the glass substrates and patterned accordingly, followed by the wet etching of the extra material. In the second step of lithography, a passivation coating of photosensitive polymer (SU8 coating of thickness 50 μm) was done over the connecting electrodes for their isolation; thus, only the sensor part of the electrodes was exposed to the analyte. The cloning cylinder working as an electrolyte reservoir was aligned and glued around the electrodes with PDMS, as shown in Fig. 2. The optical image of the final fabricated device is shown in the Fig. 3.

4 Measurement of impedance

The electrical impedance of PBS and blood was measured by using the electrochemical work station (M204, Metrohm

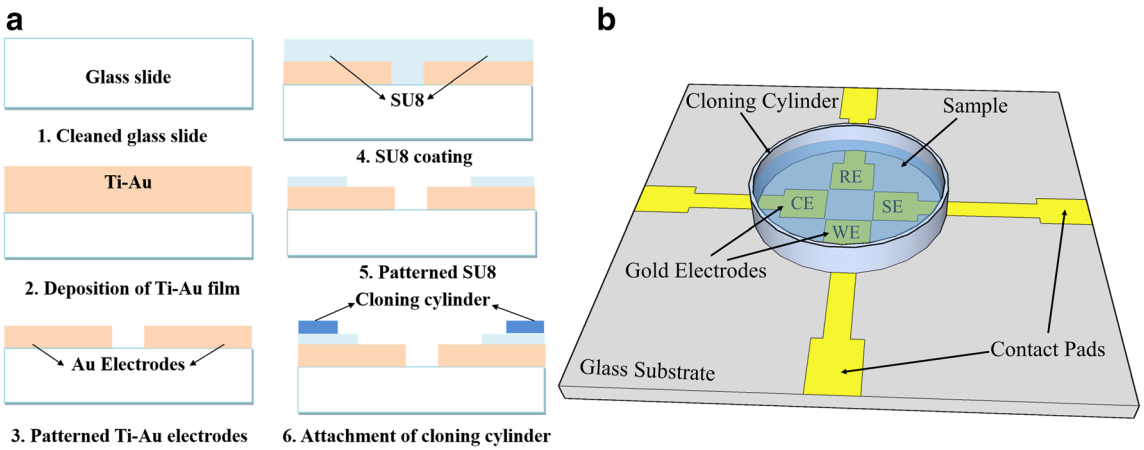

Fig. 2 a) A stepwise fabrication process flow diagram for the device b) a 3D schematic of device with cell chamber

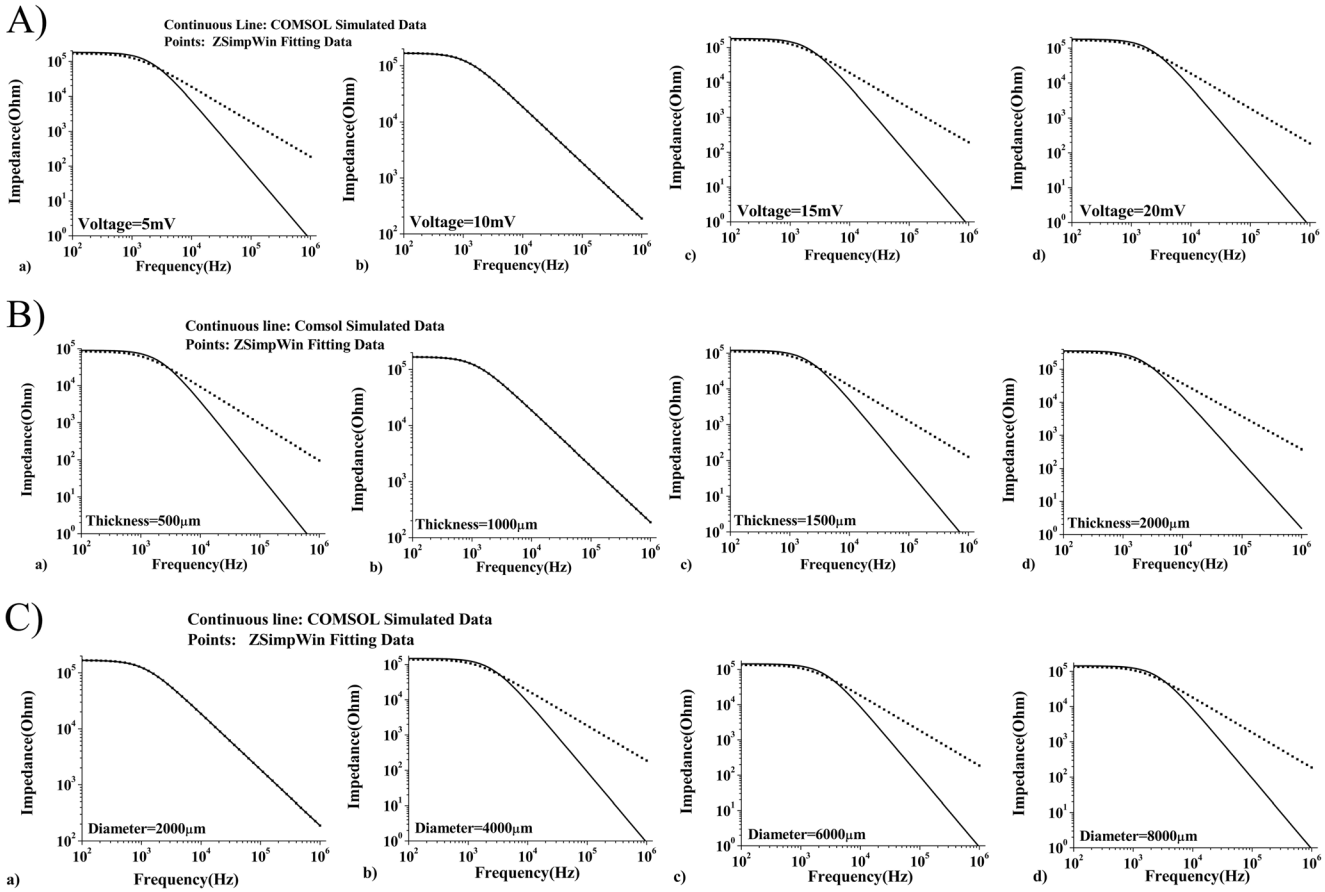

Fig. 4 Optimization of (A) Voltage, (B) PBS thickness, (C) PBS diameter

Autolab). In the present study, the sample volume of PBS and blood are taken 1 ml for each device measurement. All the analyses were performed by sweeping the frequency in a logarithmic scale from 100 Hz to 1 MHz for an actuation voltage of 10 mV. The data obtained was further exported in the ZsimpWin software to extract the electrical parameters.

5 Results and discussions

5.1 Optimization of device parameters

In the first step, the actuation voltage is optimized for the future process; for that purpose, a set of four experiments have

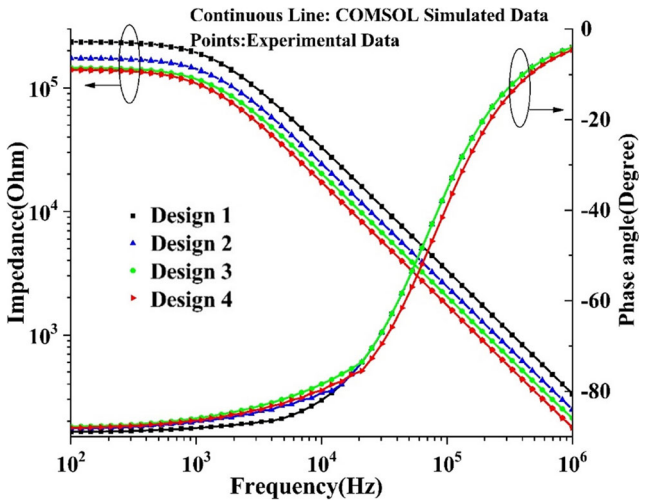

Fig. 5 Bode plot for the COMSOL simulated data and investigational results for PBS

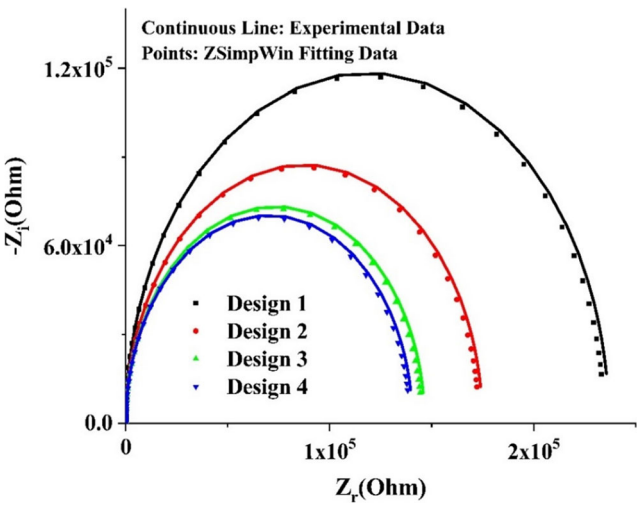

Fig. 6 Nyquist plot of experimental PBS data simulated with ZSimpWin

Table 3 Value of different electric components of the obtained circuit and RSE for PBS sample

Electric Components	Design 1		Design 2		Design 3		Design 4	
	Data	RSE%	Data	RSE%	Data	RSE%	Data	RSE%
$R_s(\Omega)$	54.36	2.12	43.23	2.33	31.74	3.01	19.36	1.02
CPE(S.Sec^n)	4.82E-10	1.24	6.53E-10	1.045	7.8E-10	2.42	9.27E-10	1.46
n	1	0.001	1	0.008	0.9998	0.007	1	0.002
$R_c(\Omega)$	2.34E5	1.06	1.73E5	1.31	1.45E5	1.02	1.39E5	1.20
χ^2(Value)	5.21E-5		1.27E-5		1.20E-5		1.77E-5	

been performed by taking the voltage 5 mV, 10 mV, 15 mV, and 20 mV respectively, as shown in Fig. 4 (A). It is evident from the figure that the ZsimpWin data matches perfectly with the simulated data for 10 mV input voltage. Therefore, for future experiments, the actuation voltage will be taken as 10 mV.

The second step is to optimize the PBS thickness for the process; a similar process is done with thickness taken as 500 μm, 1000 μm, 1500 μm, and 2000 μm, respectively. From Fig. 4 (B), a perfect match can be seen between the simulated and the fitted data; thus, we can conclude that the 1000 μm is the optimized PBS thickness and will be taken for future experiments. Similarly, the diameter of the PBS is optimized by taking four values as 2000 μm, 4000 μm, 6000 μm, and 8000 μm, respectively. It is evident from Fig. 4 (C) that the 2000 μm is the optimized diameter for PBS to get the optimum value of impedance.

5.2 Impedance of PBS sample

The Bode plot for simulated and experimental data obtained by the characterization of the device with the PBS sample is as shown in Fig. 5.

It can be seen that the total impedance decreases with the increase of the frequency, whereas the phase increases signifying the capacitive effect of the device. The electrolyte impedance and polarization electrode impedance combined gives the total impedance of the sensor. Since polarization impedance is inversely proportional to the electrode area; therefore, the electrode with the smallest area shows higher impedance and vice versa. The Design 4 geometry has a lower polarization impedance and electrolytic impedance as it allows more charge to flow through its surface. The percentage of error (RSE %) of impedance data for each design remains below 5%, which is satisfactory by nature, as depicted in previous literature (Pradhan et al. 2012; Pradhan et al. 2011).

5.3 Equivalent circuit fitting result

Figure 6 shows the Nyquist plot of the experimental data fitted by the ZsimpWin equivalent circuit models, as shown in Fig. 1, which fits well as the standard value of χ^2 value has been found to be 1.5×10^{-3} or less and the percentage of error (RSE %) of impedance data for each design remains below 5%. The circuit is the interpretation of the theoretical model of the

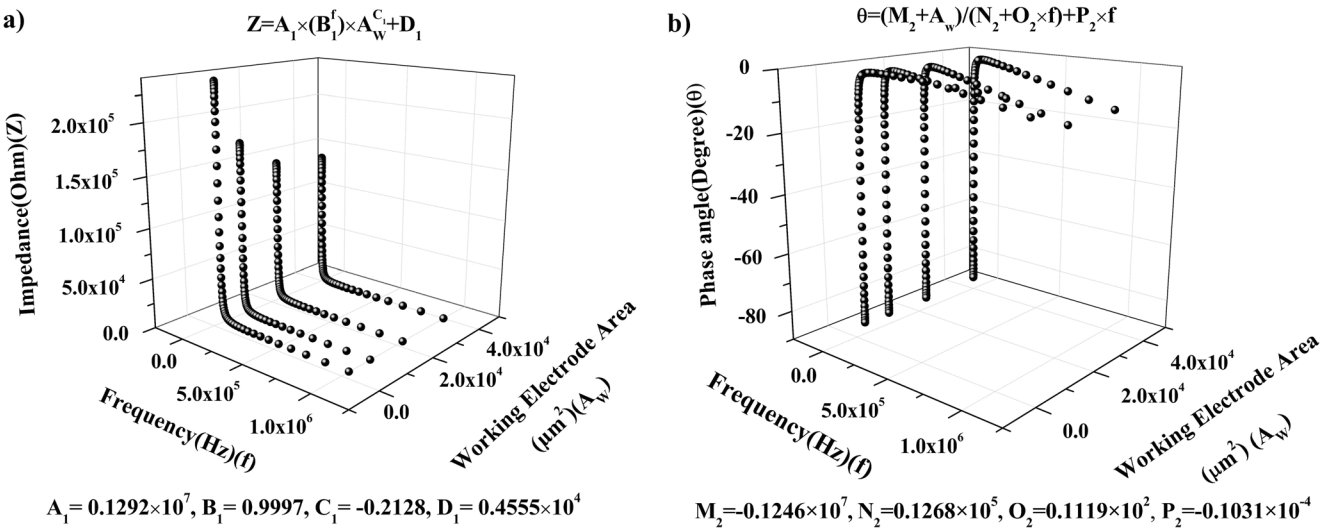

Fig. 7 Output plot showing the dependence of (a) impedance (b) phase angle of the device with the working electrode area

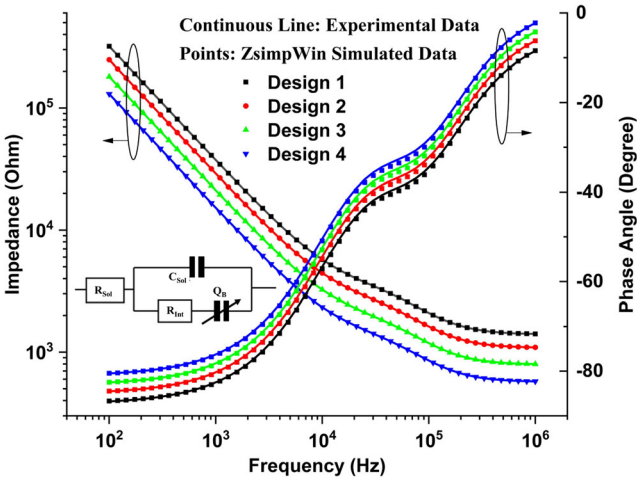

Fig. 8 Bode plot for the whole blood with an equivalent circuit (inset).

electrode/electrolyte circuit proposed by previous literature (Franks et al. 2005).

The capacitance due to the passivation coating, double-layer capacitance, and the interface capacitance behave more like constant phase elements (CPE) than an ideal capacitor. The following model parameters α and Q, as per eq. (6), express the impedance of the CPE.

$$Z = 1/Q(j\omega)^n \tag{6}$$

Here, Q is the constant, $j = \sqrt{-1}$, and n is the fractional exponent of the CPE element where the value of n varies from $0 < n < 1$. When $n = 1$, the CPE behaves like an ideal capacitor having unit capacitance, and the system is expressed by a single time-constant. When $n = 0$, CPE acts as a resistor. In this work, the value has been taken, n = 1 as per references (Pradhan et al. 2012; Pradhan et al. 2011), assuming CPE acting as a capacitor.

Table 3 shows the data and relative standard error (RSE%) of the electrical components, and it can be observed that the simulated and the experimental data has got aligned with a slight deviation, and the $\chi 2$ value is below 1.5×10^{-3} for different designs. It is evident from Table 3 that the CPE is highest in Design 4 and decreases with the decrease of electrode dimensions. In addition, the charge flow resistance decreases with the increase of electrode dimensions. This decrease may be due to more surface area, which allows more charges to flow, thus increasing the overall conductivity. However, the larger surface area also creates more contamination problems, even for the low resistive bio samples, it might not give the exact result, which thus paves the way to emphasize on the optimization of the device so that these problems can be avoided.

A mathematical expression can show the relation between electrode area with the impedance and phase angle of the optimized impedimetric sensor by plotting the magnitude of the impedance and the phase angle of the device against the variables like frequency and the area of the electrodes, as shown in Fig. 7. LAB fit curve fitting software was adopted to get a relation between different parameters, which uses the Levenberg Marquardt algorithm (Marquardt 1963) between the independent and dependent variables to find the best-fitted equation for the given data.

The mathematical relation between the magnitude of impedance (Z) and the electrode area (A_W) for the above plot has been obtained as

$$Z = A_1 \times \left(B_1^f\right) \times A_w^{C_1} + D_1 \tag{7}$$

Where the values of constants are, $A_1 = 0.1292 \times 10^7$, $B_1 = 0.9997$, $C_1 = -0.2128$, $D_1 = 0.4555 \times 10^4$ respectively. For the phase angle (θ) and the electrode area (A_w) are obtained as follows for the output plot

$$\theta = (M_2 + A_w)/(N_2 + O_2 \times f) + P_2 \times f \tag{8}$$

Where, θ is phase angle, and the constant values are $M_2 = -0.1246 \times 10^7$, $N_2 = 0.1268 \times 10^5$, $O_2 = 0.1119 \times 10^2$, $P_2 = -0.1031 \times 10^{-4}$.

The eqs. 7 and 8 are the mathematical expressions for the impedance and phase angle for optimized electrodes, obtained using the LAB fit software. Knowing the frequency and the values of the constants and the frequency of the AC signal, we can easily predict the impedance and the phase angle for the different electrode areas, which can be advantageous for selecting the perfect area for the electrode.

Table 4 Value of various electric components of the obtained circuit and RSE for the blood sample

Electrical Components	Design 1		Design 2		Design 3		Design 4	
	Data	RSE (%)	Data	RSE (%)	Data	RSE (%)	Data	RSE (%)
R_S (Ω)	1414	0.41	1096	0.37	800	0.33	576	0.36
C_S (Fs^{n-1})	1.19E-9	1.57	1.54E-9	0.90	2.11E-9	1.01	2.93E-9	0.85
R_I(Ω)	3514	2.05	2724	1.34	1989	1.83	1432	1.37
Q_M (Fs^{n-1})	6.58E-9	1.45	8.49E-9	2.11	1.16E-8	1.28	1.61E-8	1.02
n	0.91	0.17	0.91	0.14	0.91	0.10	0.91	0.03
χ^2 value	1.24E-4		1.17E-4		1.10E-4		1.08E-4	

5.4 Impedance of blood sample

In this context, the blood sample was collected in a sterilized tube from institute hospital with the written consent of the person and approval from the Institutional Ethical and Biosafety Committee (BT/IHEC-IITR/2019/7525). The sample was characterized using similar variables of the experiments as PBS. Here, Fig. 8 shows the Bode plot for the characterization of the blood using the proposed fabricated devices. It is evident from the presented results that the blood has higher impedance at the lower frequency range, which in terms decreases at higher frequencies. This is due to the fact that at a lower frequency range, most of the current flows around a blood cell because the cell membrane insulates the cytoplasm. Therefore, a longer path gives rise to an increase in the overall impedance of the system. On the other hand, at higher frequencies, the current easily passes through the cell as the membrane becomes more conductive at this frequency range. Therefore, the current conduction mechanism in the blood is a function of the cytoplasm complex impedance, as depicted by Fig. 8.

The equivalent circuit shown in Fig. 8 (inset) is used to extract the electrical parameters, as described in Table 4. In the equivalent circuit of the blood, the conductive cytoplasm can be treated as the resistor (R_{int}), the doubled layered cell membrane is equivalent to the dielectric of a capacitor (Q_B), R_{sol} demonstrates the bulk resistance offered by the extracellular solution. In contrast, the solution capacitance, $C_{sol,}$ depicts the dielectric property of the water present in the blood sample.

From Table 4, it is evident that the value of CPE increases with the increase in the electrode dimensions. Therefore, design 4 has the highest value of CPE in all the proposed electrodes. Here, the value of χ^2 varies from 1.24 E-4 to 1.08E-4, which demonstrates the validity of the model. Furthermore, the value of relative standard error (RSE%) was way below 5% for the current experiment (Pradhan et al. 2019; Zhbanov and Yang 2017; Tran et al. 2018).

6 Conclusions

In this paper, the optimization and the characterization of four electrode-based impedimetric sensors have been demonstrated. Different parameters of the electrode have been varied in order to get the optimized design, and the same was further fabricated with gold as electrode material on a glass substrate with a PBS solution as the electrolyte. A frequency range of 100 Hz to 1 MHz was applied to the fabricated device, and the outputs were compared for the COMSOL simulated output and the experimental output. The increase of the impedance with the decrease of the frequency was observed. The ZsimpWin software extracts the equivalent circuit of the device's electrochemical system, as well as the error percentage (RSE) of the device. In addition, a mathematical relation was also obtained from this optimized design between the impedance, phase angle, and electrode geometry, which will further help for a better understanding of the bio-impedance of living cells. Later, the blood sample was characterized using the optimized parameters, and the results were highly encouraging for cell diagnosis purposes.

Acknowledgments The authors acknowledge the Department of Biotechnology, Government of India (BT/PR 25095/NER/95/1011/2017). RP and A.K. are thankful to the Ministry of Education (MOE) for the fellowship. Department of Metallurgical and Materials Engineering and Institute Instrumentation Centre of Indian Institute of Technology Roorkee are sincerely acknowledged for providing the various analytical facilities.

Funding Department of Biotechnology, Government of India (BT/PR 25095/NER/95/1011/2017).

Data availability (NA)

Compliance with ethical standards

Conflict of interest None.

Ethics approval Approval from the Institutional Ethical and Biosafety Committee (BT/IHEC-IITR/2019/7525) for the collection of the blood sample.

Consent to participate The ethical approval included the written consent of the person.

Consent for publication (Y)

Code availability (NA)

References

W. Franks, I. Schenker, P. Schmutz, A. Hierlemann, Impedance characterization and modeling of electrodes for biomedical applications. IEEE Trans. Biomed. Eng. **52**, 1295–1302 (2005)

T.M. Curtis, M.W. Widder, L.M. Brennan, S.J. Schwager, W.H. van der Schalie, J. Fey, N. Salazar, A portable cell-based impedance sensor for toxicity testing of drinking water. Lab Chip **9**, 2176–2183 (2009)

S. Kumar, Ashish, S. Kumar, S. Augustine, S. Yadav, B.K. Yadav, R.P. Chauhan, A.K. Dewan, B.D. Malhotra, Effect of Brownian motion on reduced agglomeration of nanostructured metal oxide towards development of efficient cancer biosensor. *Biosens. Bioelectron* **102**, 247–255 2018/04/15/ (2018a)

J. Hong, K. Kandasamy, M. Marimuthu, C.S. Choi, S. Kim, Electrical cell-substrate impedance sensing as a non-invasive tool for cancer cell study. Analyst **136**, 237–245 (2011)

O. Láng, L. Kőhidai, J. Wegener, Label-free profiling of cell dynamics: A sequence of impedance-based assays to estimate tumor cell invasiveness *in vitro*. *Experiment Cell Res* **359**, 243–250, 2017/10/01/ (2017)

R. Pradhan, S. Rajput, M. Mandal, A. Mitra, and S. Das, Electric cell–substrate impedance sensing technique to monitor cellular behaviours of cancer cells. *RSC Adv* **4**, 9432–9438 (2014a)

A. Kalkal, R. Pradhan, S. Kadian, G. Manik, G. Packirisamy, Biofunctionalized Graphene Quantum Dots Based Fluorescent

Biosensor toward Efficient Detection of Small Cell Lung Cancer. *ACS Appl Bio Mater* **3**, 4922–4932, 2020/08/17 (2020)

C. Xiao, B. Lachance, G. Sunahara, J.H.T. Luong, An in-depth analysis of electric cell-substrate impedance sensing to study the attachment and spreading of mammalian cells. Anal. Chem. **74**, 1333–1339 (2002)

L. Wang, L. Wang, H. Yin, W. Xing, Z. Yu, M. Guo, J. Cheng, Real-time, label-free monitoring of the cell cycle with a cellular impedance sensing chip. *Biosens Bioelectron* **25**, 990–995, 2010/01/15/ (2010)

R. Pradhan, M. Mandal, A. Mitra, S. Das, Monitoring cellular activities of cancer cells using impedance sensing devices. *Sens Actuators B Chem* **193**, 478–483 (2014b)

X. Huang, D. W. Greve, D. D. Nguyen, and M. M. Domach, Impedance Based Biosensor Array for Monitoring Mammalian Cell Behavior, in *Proceedings of IEEE Sensors*, 304–309 (2003)

I. Giaever, C.R. Keese, A morphological biosensor for mammalian cells. *Nature* **366**, 591–592, 1993/12/01 (1993)

R. Pradhan, M. Mandal, A. Mitra, and S. Das, Assessing cytotoxic effect of ZD6474 on MDA-MB-468 cells using cell-based sensor. *IEEE Sens J* **14**, 1476–1481 (2014c)

Y. An, T. Jin, F. Zhang, P. He, Electric cell-substrate impedance sensing (ECIS) for profiling cytotoxicity of cigarette smoke. *J Electroanal Chem* **834**, 180–186, 2019/02/01/ (2019)

R. Pradhan, S. Rajput, M. Mandal, A. Mitra, S. Das, Frequency dependent impedimetric cytotoxic evaluation of anticancer drug on breast cancer cell. *Biosens Bioelectron* **55**, 44–50 (2014d)

R. Szulcek, H. J. Bogaard, and G. P. J. J. van Nieuw Amerongen, Electric cell-substrate impedance sensing for the quantification of endothelial proliferation, barrier function, and motility, e51300, (2014)

K. Benson, S. Cramer, H.-J. J. F. Galla, and B. o. t. CNS, Impedance-based cell monitoring: barrier properties and beyond **10**, 5, (2013)

T. Schmiedinger, S. Partel, T. Lechleitner, O. Eiter, D. Hekl, S. Kaseman, P. Lukas, J. Edlinger, J. Lechner, T. Seppi, Interdigitated aluminium and titanium sensors for assessing epithelial barrier functionality by electric cell-substrate impedance spectroscopy (ECIS). *Biomed Microdev* **22**, 30, 2020/04/24 (2020)

F. Cavallini, M. Tarantola, ECIS based wounding and reorganization of cardiomyocytes and fibroblasts in co-cultures. *Prog Biophys Mol Biol* **144**, 116–127, 2019/07/01/ (2019)

I. Giaever, C.R. Keese, Monitoring fibroblast behavior in tissue culture with an applied electric field. Proc. Natl. Acad. Sci. **81**, 3761 (1984)

I. Giaever, C.R. Keese, Micromotion of mammalian cells measured electrically. Proc. Natl. Acad. Sci. **88**, 7896–7900 (1991)

I. Giaever and C. R. Keese, Attachment and spreading of mammalian cells *in vitro*, in Soft Condensed Matter: Configurations, Dynamics and Functionality, ed: Springer, pp. 101–109 (2000)

V. Raicu, A. Popescu, Cell Membrane: Structure and Physical Properties, in Integrated Molecular and Cellular Biophysics, Springer, pp. 73–99 (2008)

B.-Y. Chang, S.-M. Park, Electrochemical impedance spectroscopy. *Annu Rev Anal Chem* **3**, 207–229 (2010)

N. Hu, J. Zhou, K. Su, D. Zhang, L. Xiao, T. Wang, P. Wang, An integrated label-free cell-based biosensor for simultaneously monitoring of cellular physiology multiparameter *in vitro*. *Biomed Microdev* **15**, 473–480, 2013/06/01 (2013)

J.J. Ackmann, Complex bioelectric impedance measurement system for the frequency range from 5 Hz to 1 MHz. *Annals of Biomedical Engineering* **21**, 135–146, 1993/03/01 (1993)

S. Kumar, S. Kumar, S. Augustine, S. Yadav, B. K. Yadav, R. P. Chauhan, A. K. Dewan, B. D. J. B. Malhotra, and bioelectronics, "Effect of Brownian motion on reduced agglomeration of nanostructured metal oxide towards development of efficient cancer biosensor," **102**, 247–255, (2018b)

R. Pradhan, A. Mitra, and S. Das, Impedimetric characterization of human blood using three-electrode based ECIS devices. *J Electr Bioimpedance* **3**, pp. 12–19 (2019)

M. E. Orazem and B. Tribollet, *Electrochemical impedance spectroscopy*: John Wiley & Sons, (2017)

G. J. Brom-Verheijden, M. H. Goedbloed, and M. A. Zevenbergen, A Microfabricated 4-Electrode Conductivity Sensor with Enhanced Range, in *Multidisciplinary Digital Publishing Institute Proceedings*, 797 (2018)

D.-H. Xia, S. Song, Y. Behnamian, W. Hu, Y.F. Cheng, J.-L. Luo, F. Huet, Review—Electrochemical Noise Applied in Corrosion Science: Theoretical and Mathematical Models towards Quantitative Analysis. *J Electrochem Soc* **167**, 081507, 2020/05/05 (2020)

T.H. Park, M.L. Shuler, Integration of Cell Culture and Microfabrication Technology. *Biotechnol Prog* **19**, 243–253, 2003/01/01 (2003)

R. Pradhan, A. Mitra, S. Das, Characterization of Electrode/Electrolyte Interface of ECIS Devices. *Electroanal* **24**, 2405–2414, 2012/12/01 (2012)

V. Srinivasaraghavan, J. Strobl, D. Wang, J.R. Heflin, M. Agah, A comparative study of nano-scale coatings on gold electrodes for bioimpedance studies of breast cancer cells. *Biomed Microdev* **16**, 689–696, 2014/10/01 (2014)

Y.-T. Lai, Y.-S. Chu, J.-C. Lo, Y.-H. Hung, C.-M. Lo, Effects of electrode diameter on the detection sensitivity and frequency characteristics of electric cell-substrate impedance sensing. *Sens Actuators B: Chem* **288**, 707–715, 2019/06/01/ (2019)

J. Huang, Y. Zhang, J. Wu, Review of non-invasive continuous glucose monitoring based on impedance spectroscopy. *Sens Actuators A: Phys* **311**, 112103, 2020/08/15/ (2020)

D. Ianni Filho, I. d. F. S. F. Boin, A. Yamanaka, Bioimpedance: New Approach to Non-Invasive Detection of Liver Fibrosis - a Pilot Study. J Arquivos de Gastroenterologia, **55**, 2–6 (2018)

T.K. Bera, Bioelectrical Impedance Methods for Noninvasive Health Monitoring: A Review. *J Med Eng* **2014**, 381251, 2014/06/17 (2014)

D. Padmaraj, J.H. Miller, J. Wosik, W. Zagozdzon-Wosik, Reduction of electrode polarization capacitance in low-frequency impedance spectroscopy by using mesh electrodes. *Biosens Bioelectron* **29**, 13–17, 2011/11/15/ (2011)

D. T. Price, A. R. A. Rahman, S. Bhansali, Design rule for optimization of microelectrodes used in electric cell-substrate impedance sensing (ECIS). *Biosens Bioelectron* **24**, 2071–2076 (2009)

M.-H. Wang, L.-S. Jang, A systematic investigation into the electrical properties of single HeLa cells via impedance measurements and COMSOL simulations. *Biosens Bioelectron* **24**, 2830–2835, 2009/05/15/ (2009)

R. Pradhan, A. Mitra, and S. Das, Simulation of three electrode device for bioimpedance study using COMSOL Multiphysics, in *2010 International Conference on Systems in Medicine and Biology*, 37–40 (2010)

R. Pradhan, A. Mitra, and S. Das, Characterization of electrode/electrolyte interface for bioimpedance study, in *IEEE Technology Students' Symposium*, 275–280 (2011)

B. A. Boukamp, *Equivalent circuit : (equivcrt.pas) : users manual*. Enschede: University of Twente, Department of Chemical Technology, (1989)

D.W. Marquardt, An algorithm for least-squares estimation of nonlinear parameters. J soc Ind Appl Math **11**, 431–441 (1963)

A. Zhbanov, S. Yang, Electrochemical impedance spectroscopy of blood for sensitive detection of blood hematocrit, sedimentation and dielectric properties. Anal. Methods **9**, 3302–3313 (2017)

A.K. Tran, A. Sapkota, J. Wen, J. Li, M. Takei, Linear relationship between cytoplasm resistance and hemoglobin in red blood cell hemolysis by electrical impedance spectroscopy & eight-parameter equivalent circuit. *Biosens Bioelectron* **119**, 103–109, 2018/11/15/ (2018)